*SF2A 2013*
*L. Cambrésy, F. Martins, E. Nuss and A. Palacios (eds)*

# A STUDY OF THE RED SUPERGIANT BETELGEUSE AT HIGH ANGULAR RESOLUTION

M. Montargès[1], P. Kervella[1], G. Perrin[1] and K. Ohnaka[2]

**Abstract.** Betelgeuse ($\alpha$ Ori) is a M2Iab star, prototype for the red supergiant class. These stars contributes to the chemical enrichment of the interstellar medium (ISM) through their heavy mass loss and thanks to the IIP type supernova of whom they are the progenitors. With its proximity ($\sim$ 130 pc) and thus of its large apparent diameter ($\sim$ 42 mas), Betelgeuse is a good candidate for a detailed study of the atmosphere of a red supergiant

Our analysis of VLTI/AMBER data allowed to characterize the close environment of the star: its molecular envelope (MOLsphere). Using a thin layer model at le Local Thermodynamical Equilibrium (LTE), we obtained its angular diameter, temperature as well as the column densities for water vapor and carbon monoxide (CO). For the K band continuum, we reconstructed a one dimension image (profile) and we quantified the inhomogeneities of the photosphere.

Keywords: infrared: stars – techniques: interferometric – stars: supergiants – stars: late-type – stars: atmospheres – stars: individual: Betelgeuse

## 1 Introduction

Massive stars as Betelgeuse are the chemical laboratories of the Galaxy: when they become supernovae, they synthesize heavy elements. Even during their supergiant phase, they participate to the chemical evolution of the ISM with their heavy mass loss. Material is ejected from the star and is becoming more and more complex as it is cooling, forming molecules and dust.

Betelgeuse has been regularly observed for a century. Many significant results were obtained in the last decade. The circumstellar environment (CSE) of the star was heavily explored: Tsuji (2000) proposed a molecular envelope to fit their observations (the MOLsphere), its characteristics and its composition were computed by Perrin et al. (2004, 2007) using IOTA and VLTI/MIDI. Using VLT/NACO and VLT/VISIR Kervella et al. (2009, 2011) observed the dusty envelope of the star up to several tens of stellar radii. Meanwhile, Ohnaka et al. (2011) observed with VLTI/AMBER for the first time the dynamics of the MOLsphere and particularly motion of CO. The photosphere was also investigated: Haubois et al. (2009) observed two bright spots with the IOTA interferometer in the H band.

Yet, the process which triggers the mass loss has not yet been unveiled. The inhomogeneous shape of the circumstellar envelope and the link between each layer is also unknown and still requires further studies. We focus here on the close ($\sim 1.2R_\star$) molecular layer composed of CO and water vapor: we investigate its size and composition (Sect. 3) we also analyze the shape of the photosphere (Sect. 4).

## 2 Observations and data reduction

### 2.1 Observations

Betelgeuse was observed with the ESO Very Large Telescope Interferometer (VLTI, Haguenauer et al. 2010) using the Astronomical Multi-BEam combineR, AMBER (Petrov et al. 2007) on January and February 2011. We used the medium spectral resolution of the instrument ($R = \frac{\lambda}{\Delta\lambda} \sim 1500$) in the H band from 1.45 to 1.80 $\mu$m

[1] LESIA, Observatoire de Paris, CNRS, UPMC, Université Paris-Diderot, 5 place Jules Janssen, 92195 Meudon, France
[2] Max-Planck-Institut für Radioastronomie, Auf dem Hügel 69, 53121 Bonn, Germany

and in the K band from 2.1 to 2.45 $\mu$m. AMBER recombines the light from two or three telescopes, either Auxiliary Telescopes (ATs) of 1.8 m of diameter or Unit Telescopes (UTs) of 8.2 m. Our observations were performed with the ATs in the E0-G0-H0, E0-G0-I1 and G0-H0-I1 configurations of the VLTI.

Data from January 1st were obtained to get a suitable configuration of the instrument and thus are not relevant for our work here.

### 2.2 *Data Reduction*

We reduced the data using the AMBER data reduction software also know as *amdlib* in its version 3.0.3 (Tatulli et al. 2007). This package produces the interferometric observables which give us information about the object's Fourier transform: the visibilities are directly its amplitude and the differential phases (DP) indicate the photocenter shift in a spectral line compared to the continuum and the closure phase (CP) is defined as the sum of the three phases along the close triangle formed by the three baselines: $\phi_{\mathrm{CP}} = \phi_{12} + \phi_{23} + \phi_{31}$. This last observable is independent from the atmospheric perturbations and indicates asymmetries in the object.

As Betelgeuse is one of the brightest source of the infrared sky and has one of the bigger angular diameter for a star, we had to use a particular reduction method to estimate the error bars and discriminate among standard and corrupted files. This procedure is described in Montargès et al. (2013). The AMBER pipeline does not include the spectral calibration : we used the telluric lines in our hotter calibrator (HR-1543, spectra type F6V) to perform it.

## 3 Model fitting

### 3.1 *K band*

The K band spectrum is clearly divided in two parts: the continuum domain ($\lambda < 2.245$ $\mu$m) where we are mostly sensitive to the star photosphere and the absorption band domain ($\lambda > 2.245$ $\mu$m) where are located CO and water vapor absorption band revealing the MOLsphere.

#### 3.1.1 Continuum analysis ($\lambda < 2.245$ $\mu$m)

The continuum data allow us to estimate the angular diameter of the star. We use two different models: the uniform disk (UD) and the power-law limb-darkened disk (LDD) described in Hestroffer (1997). As we are only interested in the shape of the star at large scale (the diameter) we only use the low spatial frequency data (first lobe of the visibility function: $f < 50$ arcsec$^{-1}$). The results of the fits are summarized in Table 1 and the corresponding visibility functions are plotted on the left pannel of Fig. 1 together with the data.

**Table 1.** Best fit values for the uniform disk ($I = I_0$) and limb-darkened disk ($I = I_0\mu^\alpha$) models.

| Model | $\theta$ (mas) | $\alpha$ | $\chi^2$ |
|---|---|---|---|
| UD | $41.01 \pm 0.02$ | - | 5.27 |
| LDD | $42.28 \pm 0.07$ | $0.155 \pm 0.009$ | 4.89 |

Townes et al. (2009) reported a significant decrease of the apparent diameter of Betelgeuse from their 11 $\mu$m observations, Ohnaka et al. (2011) analyzed the evolution of the K band diameter of the star along the same period using results from Dyck et al. (1992), Perrin et al. (2004) and Ohnaka et al. (2009, 2011). They saw no evidence for a strong variation. On the right pannel of Fig. 1 , we added our result at the end of this evolution of the K band diameter and distinguished between the data including only the continuum and the whole K band. Clearly, the star appears bigger when considering all the K band: this comes from the contribution of the MOLsphere in the CO and water vapor absorption bands at the highest wavelengths of this domain. Our measurement indicates again that the size of Betelgeuse remains constant over time.

#### 3.1.2 Absorption bands ($\lambda > 2.245$ $\mu$m)

As we previously said, wavelengths longer than 2.245 $\mu$m contains CO and water vapor absorption lines which allow us to probe the MOLsphere. We model this structure by a single thin layer containing the two molecules at the local thermodynamical equilibrium (LTE) whom lines are computed with the linelist from Goorvitch

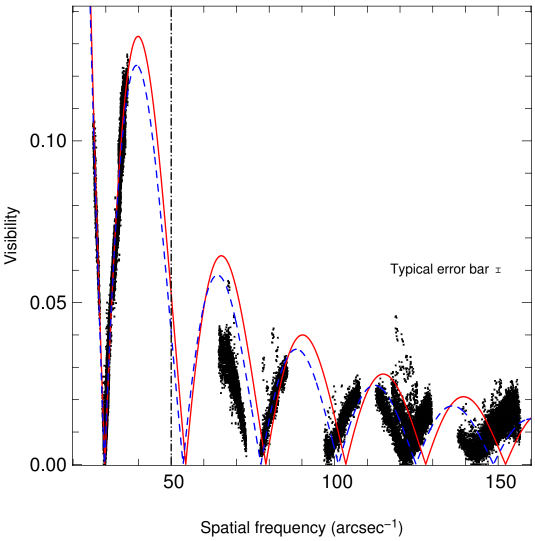


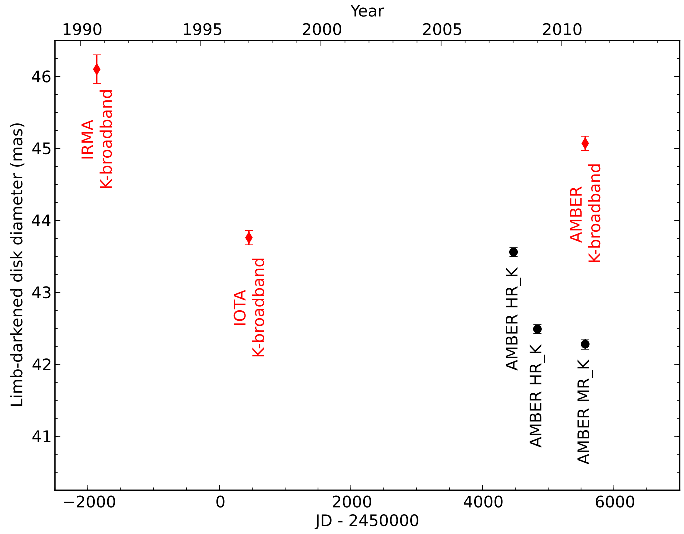


**Fig. 1. Left:** Best fit model of the continuum data. AMBER continuum data in black. The red continuous curve represent the best fit uniform disk model and the blue dashed curve represent the best fit power-law type limb-darkened model. The dashed-doted black vertical line represents the upper limit of the spatial frequencies considered for our UD/LDD fits. **Right:** Overview of limb-darkened disk measurements of Betelgeuse. The values considering only the continuum of the K band are displayed in black dots, and the K broadband measurements are in red diamonds.

(1994) and Partridge & Schwenke (1997). To model the star we used a stellar atmosphere from the Kurucz grid* (Castelli & Kurucz 2003; Kurucz 2005). The resulting analytical expression is given by :

$$I_{N_{\rm CO},N_{\rm H_2O}}(\lambda,\beta) = I_{\rm Kurucz}(\lambda)\ exp\left(\frac{-\tau(N_{\rm CO},N_{\rm H_2O};\lambda)}{\cos(\beta)}\right) + B(\lambda,T_{\rm MOL})\left[1-exp\left(\frac{-\tau(N_{\rm CO},N_{\rm H_2O};\lambda)}{\cos(\beta)}\right)\right] \tag{3.1}$$

if $\sin(\beta) \le \frac{\theta_*}{\theta_{\rm MOL}}$ and otherwise:

$$I_{N_{\rm CO},N_{\rm H_2O}}(\lambda,\beta) = B(\lambda,T_{\rm MOL})\left[1-exp\left(\frac{-2\tau(N_{\rm CO},N_{\rm H_2O};\lambda)}{\cos(\beta)}\right)\right] \tag{3.2}$$

Where the five parameters of the model are the photospheric diameter $\theta_*$, the MOLsphere diameter $\theta_{\rm MOL}$, the MOLsphere temperature $T_{\rm MOL}$, the CO and $H_2O$ column densities $N_{\rm CO}$ and $N_{\rm H_2O}$. $B(\lambda,T)$ is the Planck function, $\beta$ is the angle between the line of sight and the center of the star at the layer surface and $\tau(N_{\rm CO},N_{\rm H_2O};\lambda)$ is the MOLsphere opacity. The complete model is illustrated on Fig. 2.

Then we computed the Hankel transform to get the visibility:

$$V_\lambda(x) = \frac{\int_0^1 I(\lambda,r)J_0(rx)rdr}{\int_0^1 I(\lambda,r)rdr} \tag{3.3}$$

We did not used the data from the core of the CO band heads because amdlib was not able to fit the corresponding fringe pattern, certainly because the signal to noise ratio (SNR) was too low. Consequently, to get data points in this important wavelength domain, we included the AMBER photometry to complete our dataset. We also had to restrain ourselves to wavelengths shorter than 2.348 $\mu$m: for longer wavelengths it seems that this single model layer is not complex enough and not correctly reproducing the data (for example the spectrum on pannel right of Fig. 2). We would have had to introduce a second layer, adding 4 parameters to the fit which was already highly degenerated.

To get the best fit parameters of our data, we minimized the $\chi^2$:

$$\chi^2(T_{\rm MOL},\theta_{\rm MOL}) = \sum_{i=1}^{N}\left(\frac{Y_i - M(T_{\rm MOL},\theta_{\rm MOL},N_{\rm CO},N_{\rm H_2O};S_i)}{\sigma_i}\right)^2 \tag{3.4}$$

*http://kurucz.harvard.edu/

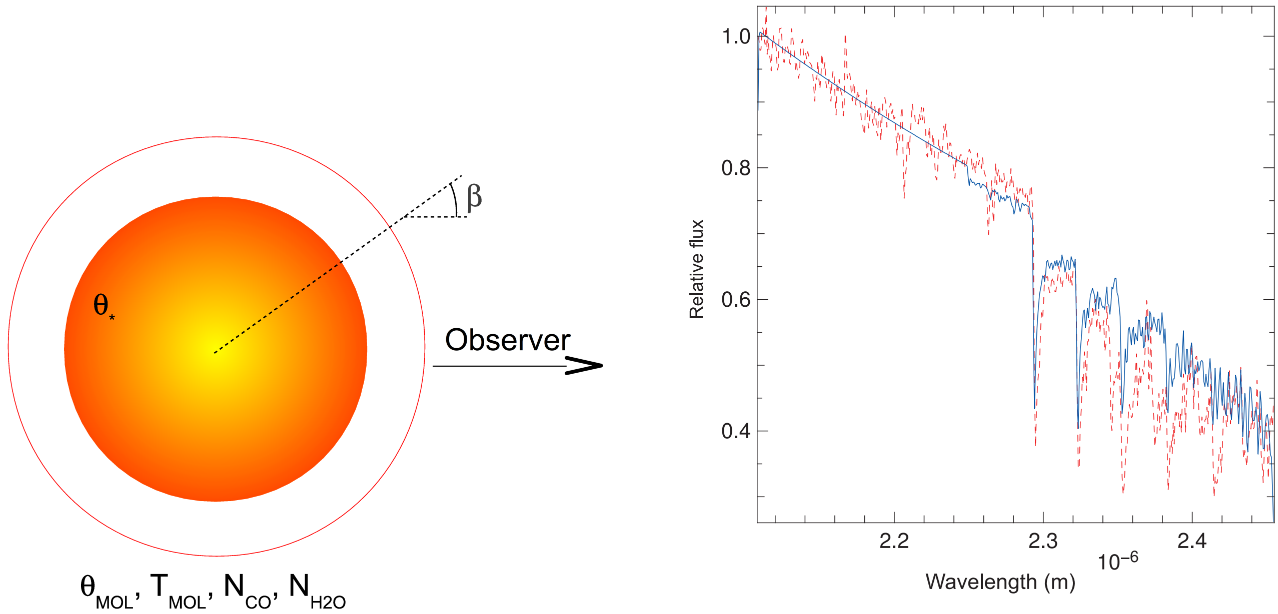


**Fig. 2. Left:** Illustration of the single layer model of the MOLsphere. $\beta$ is the angle between the radius vector and the line of sight at the layer surface. **Right:** The red dashed line is the spectrum obtained from the Betelgeuse AMBER data and the blue continuous line is the spectrum obtained from the single layer model. We used the best fit values from Table 2.

Where $S_i = B_p/\lambda$ are the sampled spatial frequencies, $Y_i$ the AMBER data (spectrum and visibilities) and $M$ the corresponding value of the model.

The five parameters of the model are not independent : the size and the temperature of the MOLsphere are of course correlated but the temperature and the two column densities and the column densities themselves are also related. Therefore we use $\chi^2$ map to find the absolute minimum of this function. First we fix the angular diameter of the star to the value of the uniform disk found in Sect. 3.1.1. Then, we fit the $N_{\rm CO}$ on a grid of $(\theta_{\rm MOL}, T_{\rm MOL})$ for a constant $N_{\rm H_2O}$. This gives us a $\chi^2$ map associated to a $N_{\rm CO}$ map. To get the equivalent maps for $N_{\rm H_2O}$ we switch round the two column densities and perform the fits again using the best fit $N_{\rm CO}$ value previously found. We iterate this process again and again until the column densities stay in their error bars. This procedure allows us to derive the best fit values for the MOLsphere parameters listed in Table 2.

**Table 2.** Best fit values with our single thin layer model of the MOLsphere

| Parameter | Value |
|---|---|
| $\theta_*$ | 41.01 mas (fixed) |
| $\rm T_{MOL}$ | $2300 \pm 120$ K |
| $\theta_{\rm MOL}$ | $51.38 \pm 1.71$ mas |
| $\rm N_{CO}$ | $3.01^{+2.00}_{-0.498} \times 10^{21}$ cm$^{-2}$ |
| $\rm N_{H_2O}$ | $3.28^{+1.73}_{-0.462} \times 10^{20}$ cm$^{-2}$ |
| $\chi^2$ | $\sim 6$ |

Remarkably, the two $\chi^2$ map for the CO and the water vapor give the same couple of parameters for the size and temperature of the MOLsphere, confirming our hypothesis of a single layer for the two molecules.

### 3.2 H band

We successfully reduced and calibrated the data in the H band but were unable to clearly distinguish continuum and absorption bands consequently it was not possible to fit the photosphere diameter. Moreover, we did not managed to reproduce all the observed absorption lines using our single layer model : more layers and/or more molecules are needed to reproduce our observations and probably a better spectral resolution.

## 4 1D profile reconstruction

Our AMBER data on Betelgeuse contain non-zero and non-$\pi$ closure phases, signatures of inhomogeneities at the star surface. Classical model fitting have proven inefficient to analyze evolving structures observed on star surfaces: one cannot guess the number and localisation of spots. Thus we use the image reconstruction algorithm MIRA (Thiébaut 2008; Renard et al. 2011) which produce an image given a prior to constrain the general shape of the star but also by fitting the data (visibilities and closure phases). Instead of simply minimizing a $\chi^2$, the algorithm minimize a cost function taking into account the classical $\chi^2$ and the prior weighted by the hyper-parameter $\mu$:

$$F_{\rm Cost} = F_{\rm Data} + \mu F_{\rm Prior} \tag{4.1}$$

The best fit limb-darkened disk model found in Sect. 3.1.1 was used as prior. We use a quadaratic regularization which discriminates the strong differences between the prior image and the reconstructed one. Other regularization methods and different values of the hyper-parameter give similar result: this strengthen the reliability of our reconstruction which represent the intensity of the star as it was observed by VLTI/AMBER.

The accuracy of the reconstructed image is partially determined by the coverage of the (u,v) plane. Our VLTI/AMBER data have a very linear (u,v) coverage which makes them more suited to a profile reconstruction along this best covered direction (azimuth 71.39°). As illustrated on Fig. 3 pannel left, we took a 8 mas wide slice along this direction on which we averaged the reconstructed intensity to obtain a profile: the result is a "smooth" convolution of the reconstructed intensity by our rectangular window. We divided this profile by the corresponding profile of the prior to obtain only the contribution of the inhomogeneities (Fig. 3, pannel right).

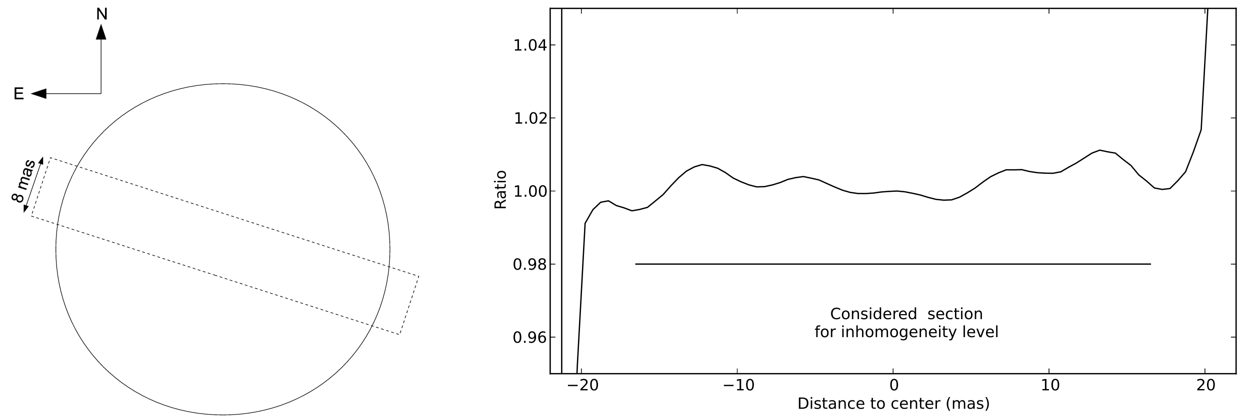


**Fig. 3. Left:** Considered fraction of the star for the averaged profile. **Right:** Ratio of the final reconstructed profile by the prior (limb-darkened disk). North-East is on the left side and South-West on the right side

To avoid edge fluctuations caused by this ratio we only consider the profile ±16.5 mas from the star center. There we computed an inhomogeneity level (defined in Eq. 4.2) of 0.809 %. It appears that we did not observe strong inhomogeneities at the star surface but we averaged the reconstructed intensity on a 8 mas wide slice meaning that we are not considering the whole star surface.

$$\tau_{\rm inhom} = \frac{I_{\rm max} - I_{\rm min}}{I_{\rm min} + I_{\rm max}} \tag{4.2}$$

## 5 Conclusions

From VLTI/AMBER data in the K band, we obtained new values for the angular diameter of $\alpha$ Ori which are consistent with the previous ones at the same wavelength. We derived characteristics of the MOLsphere, particularly we got values for the column densities of CO and water vapor. However, our analysis only covers the first two CO band heads of the K band : to get consistent results including the other absorption bands of CO, a more complex model is needed including several molecular thin layers or more probaby thick layers with parameters highly correlated. From a profile reconstruction in the continuum, by deriving an inhomogeneity level we concluded that there were no signature of strong structures on the photosphere, along our best sampled azimuthal direction.

These observations are part of a wider program aimed at understanding the shape and composition of the CSE of Betelgeuse and involving measurements in several wavelength domains and angular scales but also a monitoring at several epochs.

We are grateful to ESOs Director General Prof. Tim de Zeeuw for the allocation of observing time to our program, as well as to the Paranal Observatory team for the successful execution of the observations. The research leading to these results has received funding from the European Community's Seventh Framework Programme under Grant Agreement 226604. We acknowledge financial support from the Programme National de Physique Stellaire (PNPS) of CNRS/INSU, France. We used the SIMBAD and VIZIER databases at the CDS, Strasbourg (France), and NASAs Astrophysics Data System Bibliographic Services. This research has made use of the `AMBER data reduction package` of the Jean-Marie Mariotti Center[†]

## References

Castelli, F. & Kurucz, R. L. 2003, in IAU Symposium, Vol. 210, Modelling of Stellar Atmospheres, ed. N. Piskunov, W. W. Weiss, & D. F. Gray, 20P

Dyck, H. M., Benson, J. A., Ridgway, S. T., & Dixon, D. J. 1992, AJ, 104, 1982

Goorvitch, D. 1994, ApJS, 95, 535

Haguenauer, P., Alonso, J., Bourget, P., et al. 2010, in Society of Photo-Optical Instrumentation Engineers (SPIE) Conference Series, Vol. 7734, Society of Photo-Optical Instrumentation Engineers (SPIE) Conference Series

Haubois, X., Perrin, G., Lacour, S., et al. 2009, A&A, 508, 923

Hestroffer, D. 1997, A&A, 327, 199

Kervella, P., Perrin, G., Chiavassa, A., et al. 2011, A&A, 531, A117

Kervella, P., Verhoelst, T., Ridgway, S. T., et al. 2009, A&A, 504, 115

Kurucz, R. L. 2005, Memorie della Societa Astronomica Italiana Supplementi, 8, 14

Montargès, M., Kervella, P., Perrin, G., & Ohnaka, K. 2013, in EAS Publications Series, Vol. 60, EAS Publications Series, ed. P. Kervella, T. Le Bertre, & G. Perrin, 167–172

Ohnaka, K., Hofmann, K.-H., Benisty, M., et al. 2009, A&A, 503, 183

Ohnaka, K., Weigelt, G., Millour, F., et al. 2011, A&A, 529, A163

Partridge, H. & Schwenke, D. W. 1997, J. Chem. Phys., 106, 4618

Perrin, G., Ridgway, S. T., Coudé du Foresto, V., et al. 2004, A&A, 418, 675

Perrin, G., Verhoelst, T., Ridgway, S. T., et al. 2007, A&A, 474, 599

Petrov, R. G., Malbet, F., Weigelt, G., et al. 2007, A&A, 464, 1

Renard, S., Thiébaut, E., & Malbet, F. 2011, A&A, 533, A64

Tatulli, E., Millour, F., Chelli, A., et al. 2007, A&A, 464, 29

Thiébaut, E. 2008, in Society of Photo-Optical Instrumentation Engineers (SPIE) Conference Series, Vol. 7013, Society of Photo-Optical Instrumentation Engineers (SPIE) Conference Series

Townes, C. H., Wishnow, E. H., Hale, D. D. S., & Walp, B. 2009, ApJ, 697, L127

Tsuji, T. 2000, ApJ, 538, 801

[†]Available at `http://www.jmmc.fr/amberdrs`